

# Positional effects of phosphoserine on $\beta$ -hairpin stability†

Alexander J. Riemen and Marcey L. Waters\*

Received 3rd June 2010, Accepted 13th August 2010

DOI: 10.1039/c0ob00202j

A disruptive interaction of phosphoserine with tryptophan in peptides that autonomously fold into a  $\beta$ -hairpin structure in aqueous solution was explored in a positional context within the hairpin structure. All the peptides presented here have a serine or phosphoserine directly cross strand from a tryptophan residue in the  $\beta$ -hairpin structure. It was observed that positioning of phosphoserine-tryptophan had a less destabilizing effect if the phosphoserine was on the C-terminus as opposed to the N-terminus. Greater destabilization was observed when the phosphoserine was positioned closer to the nucleating turn sequence rather than the termini of the hairpin. Multiple phosphorylations in a hairpin designed with two cross-strand serine-tryptophan pairs resulted in a greater decrease in hairpin formation with additional incorporations of phosphoserine. The work presented here gives further insight to destabilizing phosphoserine-tryptophan interaction within the  $\beta$ -hairpin model system.

## Introduction

Phosphorylation is a key regulatory post-translational modification responsible for numerous cellular functions such as modulating cellular proliferation, macromolecule production, and gene expression.<sup>1</sup> In fact, it is estimated that one-third of all proteins in eukaryotic genome undergo reversible phosphorylation.<sup>1</sup> There are many diseases that are associated with an abnormal phosphorylation profiles such as many types of cancer and neurodegenerative diseases.<sup>1</sup> Phosphorylation acts as a molecular switch that can either activate or deactivate a protein's function. In many cases phosphorylation will alter the protein's structure, and this can cause local perturbations or long range interactions that affect its function.<sup>2</sup> However, it can be fairly difficult to study how phosphorylation affects protein structure. Model systems that investigate secondary structure stabilization can provide detailed insights into how phosphorylation affects local structure in proteins and also allows for design of novel systems that utilize phosphorylation as a molecular switching mechanism.

Previous studies in model peptide systems have shown that phosphorylation can influence local structure in a variety of ways. For example, a peptide fragment based on the PEST sequence in the E2 protein from papillomavirus showed that phosphorylation results in a destabilization of intrinsic  $\alpha$ -helix and polyproline II helix structure.<sup>3</sup> Peptides based on the bZIP protein that form  $\alpha$ -helical coiled-coils were shown to be destabilized or stabilized upon phosphorylation at different residues.<sup>4,5</sup> Phosphorylation of the proline-rich regions of the naturally disordered tau peptide induced a polyproline II helix structure.<sup>6</sup> Stabilization of  $\alpha$ -helix structure was observed when a tyrosine was phosphorylated in a peptide excised from H<sup>+</sup>/K<sup>+</sup> ATPase.<sup>7</sup> In a peptide excised from the intrinsically disordered carboxy-terminal of the H1 histone

linker protein a transition from  $\alpha$ -helix to  $\beta$ -sheet character was observed upon phosphorylation.<sup>8</sup> A study of peptides based on the N-terminal region of  $\beta$ -Catenin has shown that phosphorylation induces a more rigid and compact loop structure.<sup>9</sup> Induced loop structure upon phosphorylation was also observed in peptides based on ATF4 transcription factor protein.<sup>10</sup> A loss in loop structure was observed upon phosphorylation of a tyrosine residue in a peptide based on the activation loop of MAP kinase.<sup>11</sup> Studies of phosphorylation in *de novo* designed  $\alpha$ -helical peptides have shown that phosphorylation can stabilize  $\alpha$ -helical structure when positioned at the N-terminus or in a position to make favorable salt bridges.<sup>12,13</sup> In addition, phosphorylation has been shown to inhibit the conversion of an  $\alpha$ -helical coiled coil to an amyloid structure.<sup>14,15</sup> Indeed, it is becoming apparent that phosphorylation can induce or disrupt a variety of local secondary structures. Hierarchical multiple phosphorylation is also seen in protein post-translational modification<sup>16</sup> and hyperphosphorylation of the tau protein is observed in amyloid aggregates linked to neurodegenerative disease.<sup>6</sup> Thus it is warranted to test the effect of multiple phosphorylations in a model system like the  $\beta$ -hairpin to gain further insights into local structure perturbations.

Numerous studies on peptides that fold into a  $\beta$ -hairpin conformation have led to a thorough understanding of the design elements necessary for  $\beta$ -hairpin formation. However the effects of phosphorylation within model  $\beta$ -sheet systems has not yet been extensively explored. Previously we have described the destabilizing effect of phosphorylation of serine, threonine, and tyrosine in a  $\beta$ -hairpin system when the phosphorylated residues is in close proximity to tryptophan on the opposite strand of the  $\beta$ -hairpin.<sup>17</sup> Here we present a systematic study of the destabilizing effect of phosphorylated serines relative to their position within designed  $\beta$ -hairpin peptides.

## Results

### System Design

A set of 12-residue peptides designed to autonomously fold into  $\beta$ -hairpins in aqueous solution was used to investigate the effects

Department of Chemistry, CB 3290, University of North Carolina, Chapel Hill, NC, 27599, USA. E-mail: mlwaters@unc.edu; Fax: 919-962-2388; Tel: 919-843-6522

† Electronic supplementary information (ESI) available: NMR chemical shift assignments for all peptides and cross-strand NOEs for WTTS, WTTpS, SWLW, pSWLW, WSWL, WpSWL, WSWs and WSWpS. See DOI: 10.1039/c0ob00202j

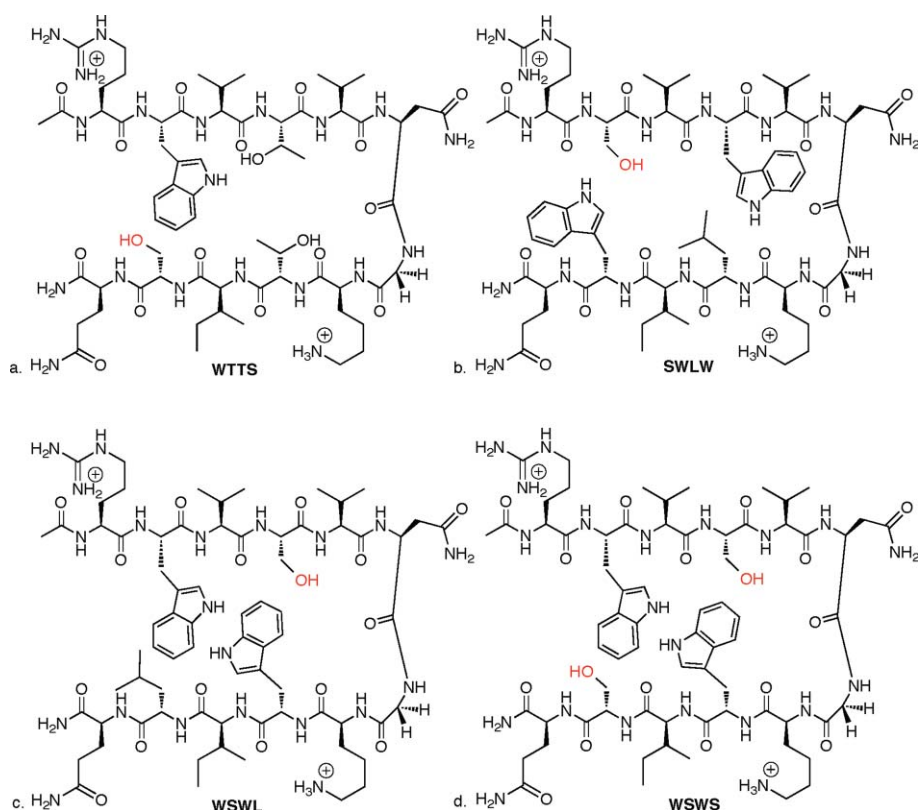


**Fig. 1** Schematic diagram of a. **WTTS**  $\beta$ -hairpin peptide, b. **SWLW**  $\beta$ -hairpin peptide, c. **WSWL**  $\beta$ -hairpin peptide d. **WSWS**  $\beta$ -hairpin peptide. The serine residues in red are replaced with phosphoserine in the phosphorylated analogs. The name of each peptide represents residues 2, 4, 9, and 11, which make up one face of the hairpin. Underlined residues in **SWLW** and **WSWL** indicate the Ser and Trp that interact.

of phosphorylation in varied positions (Fig. 1). All of the  $\beta$ -hairpin peptides contain the sequence VNGK to promote favorable type I' turn which has been shown to be significantly stabilizing in  $\beta$ -hairpin peptides.<sup>18–20</sup> The non-hydrogen bonded (NHB) sites of the  $\beta$ -hairpin peptides were varied in the four different hairpin designs to study the effects of phosphorylation. The NHB face is defined as the face of the peptide displaying side chains from the non-hydrogen bonded residue in a two-stranded  $\beta$ -sheet.<sup>21</sup> On the NHB face the side chains of residues are oriented closer to cross strand residue side chains thus giving a larger contribution to hairpin stability through side chain-side chain interactions than those residues on the hydrogen bonded (HB) face.<sup>21</sup> The **WTTS** peptide was designed to probe the effect of phosphorylation relative to which strand contains the Trp *versus* the phosphoserine (pSer). **WTTS** has Trp at position 2 while Ser or pSer is located at position 11. Thus the effect of phosphorylation can be directly compared to the previously reported **STTW** peptide<sup>17</sup> that contains Trp and Ser or pSer in the opposite strands (Fig. 1a). The **SWLW** peptide system was designed to study the effect of phosphorylation on a well folded  $\beta$ -hairpin sequence containing a serine residue at position 2 which is directly cross strand from a tryptophan at position 11 (Fig. 1b). **SWLW** utilizes a stabilizing hydrophobic cluster on the NHB face at positions 4 and 9. The **WSWL** peptide system was designed to study the effect of a phosphorylated serine cross strand from a tryptophan near the turn of a well folded  $\beta$ -hairpin containing a hydrophobic cluster on the NHB face (Fig. 1c). The **WSWS** hairpin was designed to probe the effect

of multiple phosphorylations in the same structure (Fig. 1d). **WSWS** has two cross-strand Trp-Ser interactions on the NHB face allowing for a systematic study of phosphorylation's effect on structure at each position. Unfolded control peptides were synthesized in which each peptide consisted of either residues 1–7 composing of the N-terminal arm and turn of the  $\beta$ -hairpin or residues 6–12 consisting of the C-terminal arm and turn. Cyclic control peptides were synthesized as a fully folded control for each of the  $\beta$ -hairpins. Cyclization was achieved by a disulfide bond between cysteine residues at the N and C-termini of the peptides. In each case, the peptide with pSer in place of Ser was also synthesized and studied.

### WTTS Peptide Studies

NMR was used to determine if the **WTTS** peptide and the phosphoserine containing peptide **WTTSpS** were folding into  $\beta$ -hairpin structures and to what extent they were folded. Downfield shifting of  $> 0.1$  ppm of at least three consecutive  $\alpha$ -protons ( $H\alpha$ ) along the peptide backbone relative to unfolded values indicates  $\beta$ -hairpin structure.<sup>22</sup> **WTTS** and **WTTSpS** peptides exhibit a majority of  $H\alpha$  shifts above 0.1 ppm compared to the unstructured controls (Fig. 2a), with the exception of residues Arg1, Asn6, Ser11, and Gln12. Asn6 is typically upfield shifted from unstructured control value due to the conformation it adopts in the turn. Arg1 and Gln12 are terminal residues which are usually frayed in most  $\beta$ -hairpins and give shifts below 0.1 ppm. Upfield shifting is observed

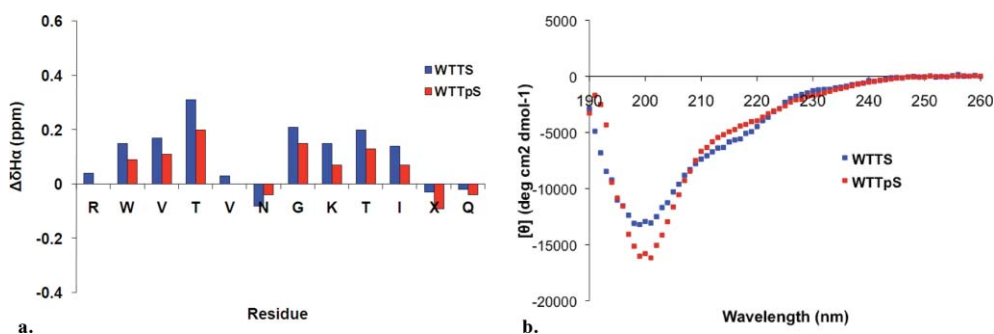


**Fig. 2** a.  $H\alpha$  chemical shift differences: **WTTS** (blue bars) and **WTTpS** (red bars) from random coil peptides in pD 7.0 buffer. Residue X is either serine (**WTTS**) or phosphoserine (**WTTpS**). The Gly bars reflect the  $H\alpha$  separation in the hairpin. b. Circular dichroism spectra comparison of **WTTS** (blue) and **WTTpS** (red) at 25 °C in 10mM sodium phosphate pH 7.0 buffer.

for Ser11 because it is cross strand from a tryptophan indole ring which shields this proton. NOESY data further confirmed that this peptide is forming the predicted  $\beta$ -hairpin structure (see ESI†).

The extent of folding of **WTTS** and **WTTpS** peptides was quantified by two methods. The first method utilizes the extent of  $H\alpha$  downfield shifting relative to random coil controls and fully folded control as previously described (see Experimental Procedures).<sup>17,23</sup> The second method utilizes the extent of the diastereotopic glycine  $H\alpha$  splitting located in the turn of the hairpin relative to glycine  $H\alpha$  splitting observed in the fully folded control (see Experimental Procedures).<sup>17,24</sup> Using these methods **WTTS** is estimated to be 35% folded and **WTTpS** is estimated to be 20% folded, giving a destabilization of approximately 0.4 kcal mol<sup>-1</sup> upon phosphorylation (Table 1). It must be noted that because these peptides are so poorly folded, the error in its value is quite large.

Circular Dichroism (CD) was also used to compare the extent of folding between **WTTS** and **WTTpS** (Fig. 2b). CD can be used for qualitative comparisons of  $\beta$ -hairpin structure, although aromatic contributions in the far-uv region can complicate interpretation of CD spectra, particularly when the aromatic residues are varied. The CD spectra of both **WTTS** and **WTTpS** exhibit a large random coil minimum at 200 nm, confirming that they are not well folded. However, at 215 nm there is a greater minimum for **WTTS** than **WTTpS**, which is indicative of  $\beta$ -sheet structure. The CD data for these peptides confirm that **WTTpS** is somewhat less folded than **WTTS**, even though the parent peptide is only modestly folded to begin with.

This destabilization is considerably less than what was observed in the previously reported **STTW** hairpin (1.3 kcal mol<sup>-1</sup>, Table 1)<sup>17</sup> indicating that orientation of the Ser-Trp interaction affects the degree of destabilization arising from phosphorylation. This is likely due to the “zipper-like” folding of these peptides, in which residue 2 is interdigitated between residues 9 and 11, whereas residue 11 only packs against residue 2. Thus, incorporating pSer at position 2 has a greater impact than at position 11.

### SWLW Peptide Studies

To further study the pSer-Trp interaction in a more stable  $\beta$ -hairpin system, **SWLW** and **pSWLW** were used. This system contains a hydrophobic cluster on the NHB face of the hairpin consisting of Trp4, Leu9, and Trp11 which increases the stability of the hairpin.

NMR characterization of **SWLW** shows that most of  $H\alpha$  shifts are downfield shifted well past 0.1 ppm with the exception of Leu 9 which is significantly upfield shifted compared to the unstructured control (Fig. 3a). This leucine is upfield shifted because of its interaction with the cross-strand Trp4, since this proton is shielded by the indole ring of the tryptophan. NOESY data confirm that this  $\beta$ -hairpin is formed in the correct register (see ESI†).

NMR characterization of **pSWLW** peptide revealed that a  $\beta$ -hairpin is still formed. A comparison of the  $H\alpha$  shifts for **pSWLW** and **SWLW** are given in Fig. 3a. A majority of  $H\alpha$  shifts for **pSWLW** are lower than **SWLW** with the exception of Trp4 and Arg1. The phosphate group may distort the hairpin in some conformation that causes these residues to be more downfield

**Table 1** Fraction folded and  $\Delta G$  of folding for peptides. Values calculated from data obtained at 25 °C, 50 mM sodium phosphate-*d*<sub>2</sub>, pD 7.0 (uncorrected), referenced to DSS

Peptide	Fraction Folded Gly Splitting <sup>a</sup>	Fraction Folded $H\alpha$ <sup>b</sup>	$\Delta G$ Folding/kcal mol <sup>-1</sup>	$\Delta\Delta G$ Folding/kcal mol <sup>-1</sup> X-pX
<b>STTW</b> <sup>c</sup>	0.41 ( $\pm$ 0.01)	0.40 ( $\pm$ 0.04)	0.23 ( $\pm$ 0.05)	
<b>pSTTW</b> <sup>c</sup>	0.10 ( $\pm$ 0.01)	0.07 ( $\pm$ 0.02)	1.53 ( $\pm$ 0.05)	1.3 ( $\pm$ 0.1)
<b>WTTS</b>	0.37 ( $\pm$ 0.01)	0.34 ( $\pm$ 0.07)	0.4 ( $\pm$ 0.2)	
<b>WTTpS</b>	0.20 ( $\pm$ 0.01)	0.20 ( $\pm$ 0.05)	0.8 ( $\pm$ 0.2)	0.4 ( $\pm$ 0.3)
<b>SWLW</b>	0.91 ( $\pm$ 0.02)	0.9 ( $\pm$ 0.1)	-1.3 ( $\pm$ 0.3)	
<b>pSWLW</b>	0.69 ( $\pm$ 0.02)	0.6 ( $\pm$ 0.2)	-0.5 – -0.2 <sup>d</sup>	0.8–1.1
<b>WSWL</b>	0.92 ( $\pm$ 0.01)	0.9 ( $\pm$ 0.03)	-1.3 ( $\pm$ 0.2)	
<b>WpSWL</b>	0.30 ( $\pm$ 0.02)	0.5 ( $\pm$ 0.1)	0–0.5 <sup>d</sup>	1.3–1.8

<sup>a</sup> Error determined by chemical shift accuracy on NMR spectrometer. <sup>b</sup> Average of the  $H\alpha$  values from Val3, Val5, Orn8, and Ile10. The standard deviation is in parentheses. <sup>c</sup> Obtained from reference 17 <sup>d</sup> Due to ambiguity in extent of  $\beta$ -hairpin formation from Gly and  $H\alpha$  shifts, the  $\Delta G$  Folding can not be accurately calculated.

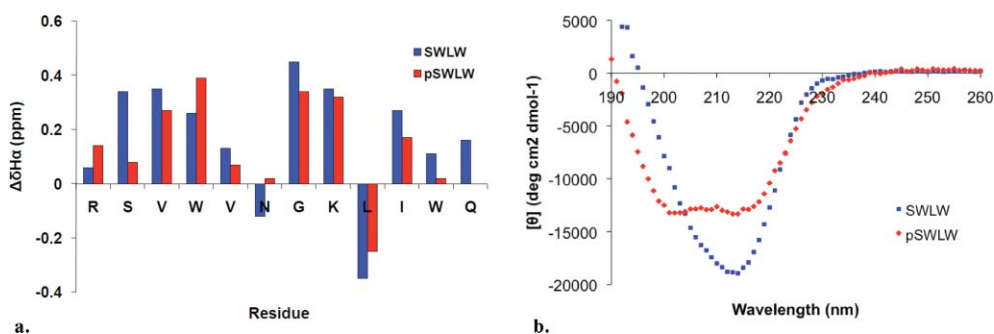


**Fig. 3** a.  $H\alpha$  chemical shift differences: **SWLW** (blue bars) and **pSWLW** (red bars) from random coil peptides in pD 7.0 buffer. The Gly bars reflect the  $H\alpha$  separation in the hairpin. b. Circular dichroism spectra comparison of **SWLW** (blue) and **pSWLW** (red) at 25 °C in 10mM sodium phosphate pH 7.0 buffer.

shifted compared to its unphosphorylated counterpart. Circular dichroism (CD) spectra for **SWLW** exhibit a minimum at 214 nm indicating  $\beta$ -sheet structure, while **pSWLW** exhibits minimum at 198 nm and a less pronounced minimum at 214 nm (Fig. 3b). A minimum at 198 nm is indicative of random coil structure, verifying that **pSWLW** is less folded than **SWLW**, which agrees well with NMR data. NOESY experiments were also performed to confirm  $\beta$ -hairpin formation. NOEs between cross strand side-chains were observed that are consistent with the expected  $\beta$ -hairpin structure (see ESI†). As expected a fewer number of NOEs were observed in the less folded **pSWLW**. **SWLW** is approximately 90% folded, with agreement between  $H\alpha$  method and the glycine splitting data (Table 1).

**pSWLW** was calculated to be between 60%–69% with some discrepancy between between  $H\alpha$  method and the glycine splitting method (Table 1). This discrepancy is most likely due to perturbations of  $H\alpha$  shifts by interaction with the phosphoserine or distortions of the  $\beta$ -hairpin structure. The  $\Delta\Delta G$  of destabilization resulting from phosphoserine in this system is estimated to be near 1.0 kcal mol<sup>-1</sup> (Table 1).

### WSWL Peptide Studies

To investigate the effect of phosphorylation-induced destabilization near the turn of a  $\beta$ -hairpin system the **WSWL** and **WpSWL** peptides were synthesized and characterized. The **WSWL** system contains the Ser cross-strand from the Trp in close proximity to the turn whereas in **STTW** and **SWLW** these residues were at the

ends of the hairpin. It has been shown that residues near the turn influence the stability of  $\beta$ -hairpins due to nucleation of the hairpin by the turn sequence and these residues are often more folded than residues near the termini.<sup>25–27</sup> We predicted that the destabilizing pSer-Trp interaction would cause a larger destabilization in well folded hairpin when this interaction is in close proximity to the turn.

$H\alpha$  chemical shift data for **WSWL** revealed a highly folded  $\beta$ -hairpin (Fig. 4) and the extent of folding was calculated to be 90% folded, with  $H\alpha$  and glycine splitting methods in good agreement (Table 1). NOESY data confirm that a  $\beta$ -hairpin is formed in the predicted register (see ESI†). The phosphorylated **WpSWL** peptide showed considerably less  $H\alpha$  downfield shifting, with the exception of phosphoserine 4 which is slightly more downfield shifted than serine 4 (Fig. 4). Very few cross strand interactions were identified for **WpSWL** by NOESY experiments which suggest a poorly folded system, in agreement with NMR chemical shifts (see ESI†). Comparison of CD spectra from **WSWL** and **WpSWL** further confirms destabilization of the hairpin fold where **WSWL** has a large minimum at 210 nm while in **WpSWL** the minimum is shifted to approximately 205 nm.

Calculation of the percent folded for **WpSWL** yielded a large discrepancy between  $H\alpha$  and glycine splitting, where  $H\alpha$  shifts gives a percent folding of 50%, but the glycine splitting calculation gives a value of 30% folded (Table 1). The low glycine splitting in this peptide may be attributed to interaction between one of the glycine hydrogens and the phosphate group where phosphate group is now in close proximity to the turn. Since the  $H\alpha$  data is

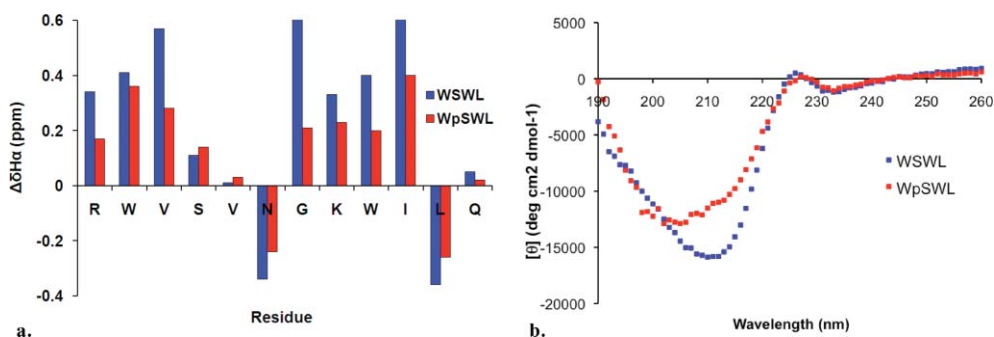


**Fig. 4** a.  $H\alpha$  chemical shift differences: **WSWL** (blue bars) and **WpSWL** (red bars) from random coil peptides in pD 7.0. The Gly bars reflect the  $H\alpha$  separation in the hairpin. b. Circular dichroism spectra comparison of **WSWL** (blue) and **WpSWL** (red) at 25 °C in 10mM sodium phosphate pH 7.0 50 buffer.

**Table 2** Fraction folded and  $\Delta G$  of folding for **WSWS** series peptides. Values calculated from data obtained at 25 °C, 50 mM sodium acetate- $d_4$ , pD 7.0 (uncorrected), referenced to DSS

Peptide	Fraction Folded (Gly) <sup>a</sup>	Fraction Folded (H $\alpha$ ) <sup>b</sup>	$\Delta G$ /kcal mol <sup>-1</sup>	$\Delta\Delta G$ /kcal mol <sup>-1</sup> (WXWZ -WSWS)
<b>WSWS</b>	0.76 ( $\pm 0.02$ )	0.70 ( $\pm 0.03$ )	-0.49 ( $\pm 0.05$ )	—
<b>WpSWS</b>	0 ( $\pm 0.02$ )	0.10 ( $\pm 0.06$ )	1.24 ( $\pm 0.4$ )	1.7
<b>WSWpS</b>	0.57 ( $\pm 0.02$ )	0.49 ( $\pm 0.02$ )	0.02 ( $\pm 0.05$ )	0.5
<b>WpSWpS</b>	0 ( $\pm 0.02$ )	0.02 ( $\pm 0.05$ )	2.22 ( $\pm 0.2$ )	2.7

<sup>a</sup> Error determined by chemical shift accuracy on NMR spectrometer. <sup>b</sup> Average of the H $\alpha$  values from Val3, Val5, Orn8, and Ile10. The standard deviation is in parentheses.

more reliable because it accounts for the folding of numerous residues, instead of just one in the glycine splitting method, it can be concluded that phosphoserine in this position causes approximately 1.3 kcal mol<sup>-1</sup> destabilization to the hairpin, which is greater than in SWLW.

### WSWS Peptide Studies

To investigate the effect of multiple phosphorylations, the **WSWS** peptide series was synthesized. Peptides **WpSWS** and **WSWpS** contain single phosphorylation modifications near the turn and near the termini, respectively. The peptide **WpSWpS** contains both phosphorylated serine residues to determine if the multiple phosphorylations decrease the stability of the hairpin more than single phosphorylation. The **WSWS** hairpin series also allowed for further investigation of positioning of the destabilizing phosphorylation interaction.

NMR characterization of the H $\alpha$  shifts showed that the **WSWS** series of peptides form  $\beta$ -hairpins with different degrees of stability (Fig. 5a). The parent peptide **WSWS** is the most stable: 76% folded based on glycine splitting and 70% based on overall H $\alpha$  shifting (Table 2). The peptide **WSWpS** is the next most stable hairpin that is approximately 50% folded based on H $\alpha$  shift and 57% based on glycine splitting. When the pSer-Trp interaction is located near the termini there is a modest destabilization of about 0.5 kcal mol<sup>-1</sup>. This destabilization is smaller than in the **STTW** and SWLW hairpin systems, but is nearly the same as in the **WTTS**, further indicating that the positioning of pSer at the C-terminus has less of a destabilizing effect than at the N-terminus. The peptide **WpSWS** is only about 10% folded indicating that the pSer-Trp interaction is much more destabilizing when in close proximity to the turn (Table 2). The extent of destabilization from phosphorylation close to the turn in **WSWS** is estimated to be 1.7 kcal mol<sup>-1</sup> (Table 2), which is greater than phosphorylation at the termini. The double phosphoserine peptide, **WpSWpS** is the least folded and has H $\alpha$  shifts close to random coil and no discernable glycine splitting, thus is considered unfolded. In addition, no long-distance NOEs were observed, suggesting poor folding of the peptide as a whole, in agreement with NMR chemical shifts.

With the **WSWS** peptide series it is difficult to make an extensive comparison of the CD data for the different phosphorylated peptides due to significant tryptophan exciton coupling that overlaps with the characteristic  $\beta$ -sheet minimum (Fig. 5b). Exciton coupling of Trp2 and Trp9 results in a minimum at 215 nm and a maximum at 229 nm, which is common for the peptides with Trp in the 2 and 9 positions.<sup>28</sup> Interestingly, the peptides that are less folded by NMR exhibit the greater exciton coupling,

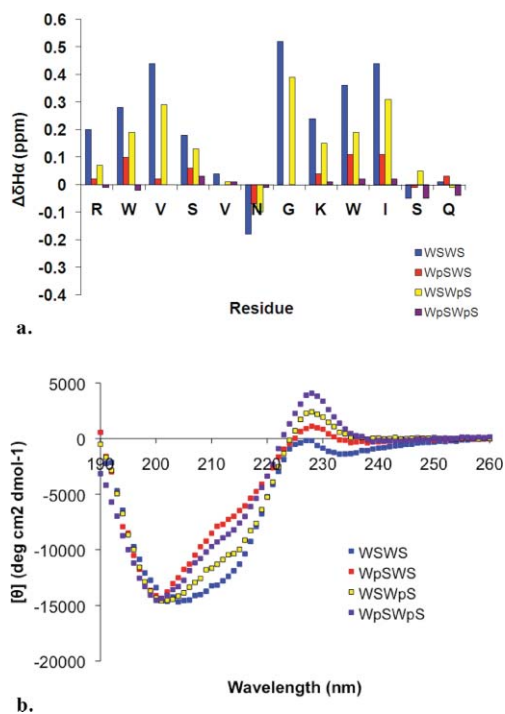


**Fig. 5** a. H $\alpha$  chemical shift differences: **WSWS** (blue), **WpSWS** (red), **WSWpS** (yellow), and **WpSWpS** (purple) from random coil peptides in pD 7.0 buffer. The Gly bars reflect the H $\alpha$  separation in the hairpin. b. Circular dichroism spectra comparison of **WSWS** (blue), **WpSWS** (red), **WSWpS** (yellow), and **WpSWpS** (purple) at 25 °C in 10mM sodium phosphate pH 7.0 buffer.

suggesting that the Trp sidechains interact with each other to a greater extent in the absence of  $\beta$ -hairpin structure.

### Conclusions

All of the peptides studied here have a structural design that positions a tryptophan directly cross-strand from serine or its phosphorylated analog. It is speculated that when the serine is phosphorylated that a repulsive anion- $\pi$  and/or charge/hydrophobic interaction results in destabilization of the overall hairpin structure.<sup>17</sup> Nonetheless, it is apparent that the destabilization caused by phosphoserine in the presence of a stabilizing hydrophobic cluster in a  $\beta$ -hairpin is highly context dependent. For example, there is a significant difference in destabilization by pSer in **WTTS** compared to **STTW** (0.4 kcal mol<sup>-1</sup> and 1.3 kcal mol<sup>-1</sup>, respectively). In **WTTS**, Ser only interacts with Trp, and so the phosphorylation will have a less pronounced effect than in **STTW**, in which Ser

interact with both Trp and Thr9. The **WSWS** peptide, which places the terminal Trp and Ser in the same positions as **WTTS**, exhibits the same degree of destabilization as **WTTS** when phosphorylated at Ser11 (0.5 kcal mol<sup>-1</sup> and 0.4 kcal mol<sup>-1</sup>, respectively), suggesting a similar contribution of the cross-strand Trp-Ser interaction in these two peptides.

The location of pSer along the N-terminal strand also has a significant effect on destabilization. The **SWLW** and **WSWL** peptides are both approximately 90% folded but exhibit different degrees of destabilization upon incorporation of phosphoserine. As expected, when the destabilizing phosphoserine is incorporated close to the nucleating turn sequence in **WpSWL**, greater destabilization is observed than for **pSWLW**. Nonetheless, it appears that **WpSWL** maintains some sort of structure along the strands, as indicated by the H $\alpha$  shifts relative to the Gly splitting and the CD spectrum with a shifted minimum.

In the case of **WSWS**, when pSer is incorporated at position 4, which is directly adjacent to the turn sequence, a larger destabilization is observed than incorporation of phosphoserine at position 11, again supporting the hypothesis that destabilization at the turn is more costly. However, as was seen in **WpSWL**, **WpWSWS** exhibits some elements of structure, particularly a Trp-Trp interaction, as indicated by the increased exciton coupling in the CD. Interestingly, this Trp-Trp interaction appears to be more favorable in **WpSWpS**, even though the peptide does not exhibit any  $\beta$ -sheet structure. Studies on the **WSWS** peptide reinforce the positional dependence of the destabilizing phosphoserine and also demonstrate that additional phosphorylation in this hairpin system results in an increased net destabilization of the fold.

In conclusion, we find consistent destabilizing effects due to phosphorylation cross-strand from Trp, but the magnitude of the effect depends on the position of the phosphorylation site. Two phosphorylations are enough to completely inhibit  $\beta$ -hairpin formation, yet a Trp-Trp interaction remains, providing insight into the significant driving force for such an interaction. These studies provide a framework for understanding how phosphorylation may impact protein structure and function. In addition, the destabilization observed from phosphoserine interacting with tryptophan lends itself as an interesting design element to the  $\beta$ -hairpin scaffold. These studies provide a framework for the development of more advanced phosphorylation controlled  $\beta$ -hairpin switching systems.

## Experimental

### Synthesis and Purification of peptides

Peptides were synthesized by automated solid phase peptide synthesis on an Applied Biosystems Pioneer Peptide Synthesizer using Fmoc protected amino acids on a PEG-PAL-PS resin from AnaSpec. Activation of amino acids was performed with HBTU, HOBT in the presence of DIPEA in DMF. Deprotections were carried out in 2% DBU (1,8 diazabicyclo[5.4.0]undec-7-ene), 2% piperidine in DMF for approximately 10 min. Extended cycles (75 min) were used for each amino acid coupling step. All control peptides were acetylated at the N-terminus with 5% acetic anhydride, 6% lutidine in DMF for 30 mins. Cleavage of the peptide from the resin was performed in 95 : 2.5 : 2.5 Trifluoroacetic acid (TFA): Ethanedithiol or Triisopropylsilane (TIPS): water for

3 h. Ethanedithiol was used as a scavenger for sulfur containing peptides. TFA was evaporated and cleavage products were precipitated with cold ether. The peptide was extracted into water and lyophilized. It was then purified by reverse phase HPLC, using a Vydac C-18 semi-preparative column and a gradient of 0 to 100% B over 40 min, where solvent A was 95 : 5 water-acetonitrile, 0.1% TFA and solvent B was 95 : 5 acetonitrile:water, 0.1% TFA. After purification the peptide was lyophilized to powder and identified with ESI-TOF mass spectroscopy.

### Cyclization of Cyclic peptides

Cyclic control peptides were cyclized by oxidizing the cysteine residues at the ends of the peptide by stirring in a 10 mM phosphate buffer (pH 7.5) in 1% DMSO solution for 9 to 12 h. The solution was lyophilized to a powder and purified with HPLC using previously described method.

### CD Spectroscopy

CD spectroscopy was performed on an Aviv 62DS Circular Dichroism Spectrophotometer. Spectra were collected from 260 nm to 185 nm at 25 °C, 1 s scanning.

### NMR Spectroscopy

NMR samples were made to a concentration of 1 mM in D<sub>2</sub>O buffered to pD 4.0 (uncorrected) with 50 mM NaOAc-d<sub>3</sub>, 24 mM AcOH-d<sub>4</sub>, 0.5 mM DSS, or pD 7.0 (uncorrected) with 50 mM KD<sub>2</sub>PO<sub>4</sub>, 0.5 mM DSS. Samples were analyzed on a Varian Inova 600-MHz instrument. One dimensional spectra were collected by using 32-K data points and between 8 to 128 scans using 1.5 s presaturation. Two dimensional total correlation spectroscopy (TOCSY) and nuclear overhauser spectroscopy (NOESY) experiments were carried out using the pulse sequences from the chempack software. Scans in the TOCSY experiments were taken 16 to 32 in the first dimension and 64 to 128 in the second dimension. Scans in the NOESY experiments were taken 32 to 64 in the first dimension and 128 to 512 in the second dimension with mixing times of 200 to 500 msec. All spectra were analyzed using standard window functions (sinbell and Gaussian with shifting). Presaturation was used to suppress the water 5 resonance. Assignments were made by using standard methods as described by Wüthrich.<sup>29</sup> All experiments were run at 298.15 K.

### Determination of Fraction Folded

To determine the unfolded chemical shifts, 7-mers were synthesized as unstructured controls and cyclic peptides were synthesized for fully folded. The chemical shifts for residues in the strand and one turn residue were obtained from each 7-mer peptide. The chemical shifts of the fully folded state were taken from the cyclic peptides. The fraction folded on a per residue bases was determined from eqn (1).

$$\text{Fraction Folded} = [\delta_{\text{obs}} - \delta_0] / [\delta_{100} - \delta_0], \quad (1)$$

where  $\delta_{\text{obs}}$  is the observed H $\alpha$  chemical shift,  $\delta_{100}$  is the H $\alpha$  chemical shift of the cyclic peptides, and  $\delta_0$  is the H $\alpha$  chemical shift of the unfolded 7-mers. The overall fraction folded for the entire peptide was obtained by averaging the fraction folded of residues Val3,

Lys8, and Ile10. These residues are in hydrogen bonded positions have been shown to be the most reliable in determining fraction folded.<sup>30</sup> The overall fraction fold was also determined using the extent of H $\alpha$  glycine splitting observed in the turn residue Gly10 given in eqn (2).

$$\text{Fraction Folded} = [\Delta\delta_{\text{Gly Obs}}]/[\Delta\delta_{\text{Gly 100}}], \quad (2)$$

where  $\Delta\delta_{\text{Gly Obs}}$  is the difference in the glycine H $\alpha$  chemical shifts of the observed, and  $\Delta\delta_{\text{Gly 100}}$  is the difference in the glycine H $\alpha$  chemical shifts of the cyclic peptides.

The  $\Delta G$  of folding at 298 K for the peptides was calculated using eqn (3) where  $f$  is the fraction folded.

$$\Delta G = -RT \ln (f/(1-f)), \quad (3)$$

## Notes and references

- 1 P. Cohen, *Eur. J. Biochem.*, 2001, **268**, 5001–5010.
- 2 L. N. Johnson and R. J. Lewis, *Chem. Rev.*, 2001, **101**, 2209–2242.
- 3 M. M. Garcia-Alai, M. Gallo, M. Salame, D. E. Wetzler, A. A. McBride, M. Paci, D. O. Cicero and G. de Prat-Gay, *Structure*, 2006, **14**, 309–319.
- 4 L. Szilak, J. Moitra and C. Vinson, *Protein Sci.*, 1997, **6**, 1273–1283.
- 5 L. Szilak, J. Moitra, D. Krylov and C. Vinson, *Nat. Struct. Biol.*, 1997, **4**, 112–114.
- 6 A. A. Bielska and N. J. Zondlo, *Biochemistry*, 2006, **45**, 5527–5537.
- 7 N. Fujitani, M. Kanagawa, T. Aizawa, T. Ohkubo, S. Kaya, M. Demura, K. Kawano, S. Nishimura, K. Taniguchi and K. Nitta, *Biochem. Biophys. Res. Commun.*, 2003, **300**, 223–229.
- 8 A. Roque, I. Ponte, J. L. R. Arrondo and P. Suau, *Nucleic Acids Res.*, 2008, **36**, 4719–4726.
- 9 S. Megy, G. Bertho, J. Gharbi-Benarous, F. Baleux, R. Benarous and J. P. Girault, *Peptides*, 2005, **26**, 227–241.
- 10 J. Pons, N. Evrard-Todeschi, G. Bertho, J. Gharbi-Benarous, R. Benarous and J. P. Girault, *Peptides*, 2007, **28**, 2253–2267.
- 11 A. A. Tokmakov, K. I. Sato and Y. Fukami, *Biochem. Biophys. Res. Commun.*, 1997, **236**, 243–247.
- 12 C. D. Andrew, J. Warwicker, G. R. Jones and A. J. Doig, *Biochemistry*, 2002, **41**, 1897–1905.
- 13 N. Errington and A. J. Doig, *Biochemistry*, 2005, **44**, 7553–7558.
- 14 M. Broncel, S. C. Wagner, C. P. R. Hackenberger and B. Kokschi, *Chem. Commun.*, 2010, **46**, 3080–3082.
- 15 M. Broncel, S. C. Wagner, C. P. R. Hackenberger and B. Kokschi, *Chem.–Eur. J.*, 2010 Early View.
- 16 P. J. Roach, *J. Biol. Chem.*, 1991, **266**, 14139–14142.
- 17 A. J. Riemen and M. L. Waters, *J. Am. Chem. Soc.*, 2009, **131**, 14081–14087.
- 18 M. Ramirez-Alvarado, F. J. Blanco and L. Serrano, *Nat. Struct. Biol.*, 1996, **3**, 604–612.
- 19 G. J. Sharman and M. S. Searle, *Chem. Commun.*, 1997, 1955–1956.
- 20 F. J. Blanco, M. A. Jimenez, J. Herranz, M. Rico, J. Santoro and J. L. Nieto, *J. Am. Chem. Soc.*, 1993, **115**, 5887–5888.
- 21 F. A. Syud, H. E. Stanger and S. H. Gellman, *J. Am. Chem. Soc.*, 2001, **123**, 8667–8677.
- 22 G. J. Sharman, S. R. Griffiths-Jones, M. Jourdan and M. S. Searle, *J. Am. Chem. Soc.*, 2001, **123**, 12318–12324.
- 23 A. J. Maynard, G. J. Sharman and M. S. Searle, *J. Am. Chem. Soc.*, 1998, **120**, 1996–2007.
- 24 S. R. Griffiths-Jones, A. J. Maynard and M. S. Searle, *J. Mol. Biol.*, 1999, **292**, 1051–1069.
- 25 M. S. Searle, *J. Chem. Soc., Perkin Trans. 2*, 2001, 1011–1020.
- 26 J. F. Espinosa, V. Munoz and S. H. Gellman, *J. Mol. Biol.*, 2001, **306**, 397–402.
- 27 S. E. Kiehna and M. L. Waters, *Protein Sci.*, 2003, **12**, 2657–2667.
- 28 A. G. Cochran, N. J. Skelton and M. A. Starovasnik, *Proc. Natl. Acad. Sci. U. S. A.*, 2001, **98**, 5578–5583.
- 29 K. Wüthrich, *NMR of Proteins and Nucleic Acids*, Wiley, New York, 1986.
- 30 F. A. Syud, J. F. Espinosa and S. H. Gellman, *J. Am. Chem. Soc.*, 1999, **121**, 11577–11578.